Supplementary information

Dispersed Ni Nanoparticles Stabilize Silicon Photoanodes for Efficient and Inexpensive Sunlight-Assisted Water Oxidation

G. Loget,*[†] B. Fabre,[†] S. Fryars,[†] C. Meriadec,[‡] and S. Ababou-Girard[‡]

[†] Institut des Sciences Chimiques de Rennes, UMR 6226 CNRS, Matière Condensée et Systèmes Electroactifs (MaCSE), Université de Rennes 1, Campus de Beaulieu, 35042 Rennes Cedex, France

[‡] Institut de Physique de Rennes, UMR 6251 CNRS, Equipe de Physique des Surfaces et Interfaces, Université de Rennes 1, Campus de Beaulieu, 35042 Rennes Cedex, France

Table of contents

1. Experimental section

1.1. Reagents

Acetone (MOS electronic grade, Erbatron from Carlo Erba) and anhydrous ethanol (RSE electronic grade, Erbatron from Carlo Erba) were used without further purification. The ultrapure water had a resistivity of 18.2 MΩ cm (Purelab Classic UV). The chemicals used for the cleaning and etching of silicon wafer pieces (30% H_2O_2, 96-97% H_2SO_4 and 50% HF solutions) were of VLSI (H_2O_2, from Sigma-Aldrich) and MOS (H_2SO_4 from BASF and HF from Sigma-Aldrich) semiconductor grade. NaOH (> 98 %, ACS reagent) was purchased from Sigma-Aldrich. Boric acid (> 99.8 %) and $NiCl_2$, 6 H_2O (99.3 %) were purchased from Alfa Aesar.

1.2. Surface preparation

All Teflon vials and tweezers used for cleaning of silicon were previously decontaminated in 3/1 v/v concentrated H_2SO_4/30% H_2O_2 at 100 °C for 30 min, followed by copious rinsing with ultrapure water. ***Caution****: the concentrated aqueous H_2SO_4/H_2O_2 (piranha) solution is very dangerous, particularly in contact with organic materials, and should be handled extremely carefully.* The *n*-type (1-5 Ω cm resistivity, phosphorus doped, double side polished, 250-275 μm thickness) (100) and p^{++}-type (0.001 Ω cm resistivity, boron doped, single side polished, 250-300 μm thickness) (100) silicon wafers were purchased from Siltronix. The wafers were cut into 1 x 2 cm² rectangles and degreased by sonication (10 min) in acetone, ethanol, and ultrapure water. The surfaces were then cleaned in 3/1 v/v concentrated H_2SO_4 /30% H_2O_2 at 100 °C for 30 min, followed by copious rinsing with ultrapure water.

1.3. Electrodeposition

Before electrodeposition, the ohmic contact was prepared as follows: *i*) the decontaminated and oxidized Si surface was freshly hydrogenated by dipping it for 2 min in 5/1 v/v ultrapure water/50% aq. HF and quickly dried under an Ar flow, *ii*) the top of the surface (≈ 1 x 0.2 cm^2) was scratched using a diamond glass cutter and a small droplet of InGa eutectic (99.99%, Alfa Aesar) was applied on the scratched surface, *iii*) a layer of silver paste (Electron Microscopy Sciences) was then carefully deposited on the InGa in order to cover it. After drying of the silver paste, the uncoated Si surface was then dipped for 2 min in 5/1 v/v ultrapure water/50% aq. HF and quickly dried under an Ar flow. The backside surface was then quickly covered with an adhesive tape to prevent electrodeposition on this side. The electrical contact was made using an alligator clip on the silver-coated InGa. The bare Si-H surface was then immersed

in the freshly prepared Ni plating solution that was composed of 0.1 M boric acid and 0.1 M $NiCl_2$, 6 H_2O in ultrapure water. For the electrodeposition, a 100 mL beaker served as a cell, the electrolyte was not deaerated and the electrolyte was not stirred. The counter electrode was a Pt plate and the reference electrode a SCE. The Ni electrodeposition was done potentiostatically by applying -1.5 V vs SCE during the desired time (typically 5 s, 20 s or 60 s). After electrodeposition, the surface was rinsed with ultrapure water and dried with an Ar stream.

1.4. Electrode fabrication

For photoelectrochemical characterization, the Ni-coated Si surfaces were further processed to fabricate electrodes. First, the adhesive tape that covered the back of the surface was carefully removed and the top contact, which was made prior to electrodeposition, was removed by cutting this part with a diamond glass cutter. An ohmic contact was established on the backside Si surface with a metal wire by first scrubbing the surface with sand paper and a diamond glass cutter and then applying a droplet of InGa eutectic. A layer of silver paste was then deposited on the contact. After drying of the silver paste, the metal wire was inserted in a glass capillary, and the electrode area (0.3 to 0.4 cm^2) was defined on the front side (the side coated with Ni) with an epoxy-based resin (Loctite 9460, Henkel) that also covered all the back of the Si surface and a part of the glass capillary in order to ensure a proper shielding of the ohmic contact. The electrode was then placed overnight at 80 °C to cure the resin.

1.5. Photoelectrochemical measurements

The cyclic voltammetry (CV) and linear sweep voltammetry (LSV) were performed in a homemade three-neck cell comprising a quartz window and gas inlets in which were inserted a KCl-saturated calomel reference electrode (SCE) that was protected from the alkaline solution by a bridge containing a saturated KCl solution and a Pt counter electrode that was separated from the rest of the cell by a glass frit. The cell was filled with a 1 M NaOH solution (measured pH = 14) and was deaerated by bubbling Ar for at least 30 min prior to experiments. The Ni-coated Si surface sealed in epoxy was disposed in front of the quartz window and used as a working electrode. The light was provided by a solar simulator (LS0106, LOT Quantum Design) equipped with an AM 1.5G filter. The power intensity of the light source, where the photoanode was located, was set to 100 mW cm^{-2} using an ILT1400 radiometer (International Light Technologies) and was measured prior to measurements with an optical power/energy meter (842-PE, Newport) coupled to a silicon photodiode (918D-SL-OD3, Newport). Electrochemical measurements were performed with a

potentiostat/galvanostat Autolab PGSTAT 302N (Eco Chemie BV) equipped with the GPES and FRA softwares. Before the experiments, the Ni-coated electrodes were cycled in 1 M NaOH under illumination by imposing several CV scans (typically from 20 to 40 scans) until the current reached stability. Fig. S8 shows a typical cycling for a *n*-Si electrode that was coated by electrodepositing Ni for 5 s. Unless specified, the CVs and LSVs reported in this work were recorded at 20 mV s^{-1}. Unless specified, the reported potentials were not corrected by the ohmic drop. The ohmic drop was determined before each experiment by measuring the impedance of the system at 100 kHz and it was found to be around 50-60 Ω. The geometrical areas of the photoelectrodes varied from 0.3 to 0.4 cm^2 and their exact value was measured using the ImageJ software, to calculate the current densities. Potentials *vs* SCE were converted into potentials *vs* reversible hydrogen electrode (RHE) using the relation:

$$E_{RHE} = E_{SCE} + 0.24 + 0.059\ \mathrm{pH} = E_{SCE} + 1.066$$

The applied bias photon-to-current efficiency (ABPE) has been determined for the best photoanode (electrodeposition time of 5 s), as shown in Figure S14. It was calculated as follows:[1]

$$ABPE = \frac{j \times (1.23 - E_{RHE})}{P_{in}} \times 100$$

with P_{in} being the power input (100 mW cm^{-2}).

1.6. Preparative-scale electrolysis

Two experimental procedures were employed for measuring the amount of produced O_2 and the faradaic efficiencies. In the first method, a preparative-scale electrolysis was performed in a homemade Hoffman cell comprising a quartz window and two closed graduated cylinders located respectively above the anolyte compartment (that contained the working electrode: Ni-coated *n*-Si with 5 s electrodeposition time) and the catholyte compartment (that contained a graphite rod counter electrode). For the interested reader, more technical details about Hoffman cell can be found in the following reference.[2] The Ni-coated *n*-Si photoanode had an area of 0.38 cm^2. First, the anolyte was saturated with O_2 by applying +1 V vs SCE for 1 h with the cylinders being open. After that, the cylinders were closed and the preparative-scale electrolysis was done at +1 V vs SCE in 1 M NaOH. During this electrolysis, evolved O_2 accumulated in the anolyte headspace and was measured *in-situ* during the electrolysis, allowing to calculate the number of moles of evolved O_2, $n_{O_2\,prod}$. The resulting chronoamperogram is shown in Fig. S9, and allowed to

determine that a total charge Q = +45.05 C was consumed after 1 h. The theoretical number of moles of O_2 was calculated as follows:

$$n_{o_2\,theo} = \frac{Q}{4F}$$

with F being the Faraday constant. The faradaic efficiency, η was then determined using the following relation:

$$\eta = \frac{n_{o_2\,prod}}{n_{o_2\,theo}} \times 100$$

In the second method, we directly compared the amount of O_2 produced by the Ni coated *n*-Si (obtained with a 5 s electrodeposition time) and a material whose faradaic efficiency is known, in this case a commercial Ni foil (Aldrich, purity of 99.98 %, area = 1.4 cm^2), that has a faradaic efficiency of 90 % in 1 M NaOH.[3] Note that the Ni foil was first cleaned by sonication in acetone, ethanol, and ultrapure water and pre-treated by imposing a current density of 20 mA during 1100 s in 1 M NaOH. Both electrolyses were performed in the exact same conditions, in a tightly-sealed homemade three-neck cell comprising a quartz window, a catholyte compartment (containing a Pt cylinder counter electrode) separated from the rest of the cell by a glass frit and a SCE reference. 35 mL of the 1 M NaOH solution was inserted in the cell that was deaerated by bubbling Ar for 1 h. The anolyte was stirred and the electrolysis was done galvanostatically by applying 25 mA for the Ni foil and 9 mA for the *n*-Si photoanode. The electrolysis was stopped after +45 C was consumed. In both cases, 50 μL of the headspace above the anolyte was manually injected into the gas chromatograph (Clarus 180, Perkin Elmer), and analyzed with a TCD detector. The results, obtained for three independent injections are shown in Fig. S10. From this data, it can be concluded that the volume of produced O_2 is slightly higher than the one evolved on the Ni plate, confirming that the faradaic efficiency is higher than 90 % on the Ni NP-decorated *n*-Si photoanode.

The turnover frequency (TOF) was calculated on the basis of the preparative-scale electrolysis shown in Figure 3b. The produced $n_{o_2\,prod}$ (for an area of 1 cm^2) was 268.4 μmol. The number of moles of the active catalytic sites, n_{Ni} , was calculated from the voltammogram shown in Figure S11. The charge density corresponding to the oxidation of Ni^{2+} to Ni^{3+}, Q_{Ni}, was determined from the area under the voltammetric wave as follows:

$$Q_{Ni} = \int_{-0.130}^{0} j(E)\, dE/V$$

with *V* being the scan rate in V s^{-1}. The calculated charge density was 2.28 x10^{-4} C, which corresponds to n_{Ni} = 2.36 x10^{-9} mol. The turnover number (TON) is defined as follows:

$$TON = \frac{n_{O_2\,prod}}{n_{Ni}}$$

and the TOF as follows:

$$TOF = \frac{TON}{t}$$

with *t* being the time of electrolysis (1 h); TOF = 1.14 x10^{5} h^{-1}.

1.7. Surface characterization

Scanning electron microscopy (SEM) was performed using a JSM 7100F (JEOL). SEM picture analysis was performed using the ImageJ software. Energy-dispersive X-ray spectroscopy was done using a Silicon Drift Detector (SDD) - X-Max (Oxford Instruments) and the AZtecEnergy software. X-ray diffraction (XRD) analysis was done on a Brucker D8 advance (operating power 40mA/40kV). XPS measurements were performed with a Mg K_{alpha} (hV) 1254 eV X-ray source, using a VSW HA100 photoelectron spectrometer with a hemispherical photoelectron analyzer, working at an energy pass of 20 eV for survey and resolved spectra. The experimental resolution was 1.0 eV.

1.8. Description of the XPS spectra

XPS analyses revealed that Ni^0 and oxidized Ni were present on the freshly-prepared surface[4] but Ni^0 was no longer detectable after the prolonged electrolysis. This confirmed that the initial Ni NPs are mainly composed of Ni^0, covered with a native oxide layer. Yet, the outermost part of the Ni NPs was oxidized during the electrolysis,[5,6] which is in very good agreement with a shielding of the Ni NPs by catalytically-active NiOOH that forms during anodic polarization, as it was observed in the CVs of Fig. S6 and Fig. S11 and reported in the literature.[5,6] Note that the peaks at 861.5 eV and 879.6 eV correspond to the Ni $2p_{3/2}$ and Ni $2p_{1/2}$ satellites.

2. Supplementary figures

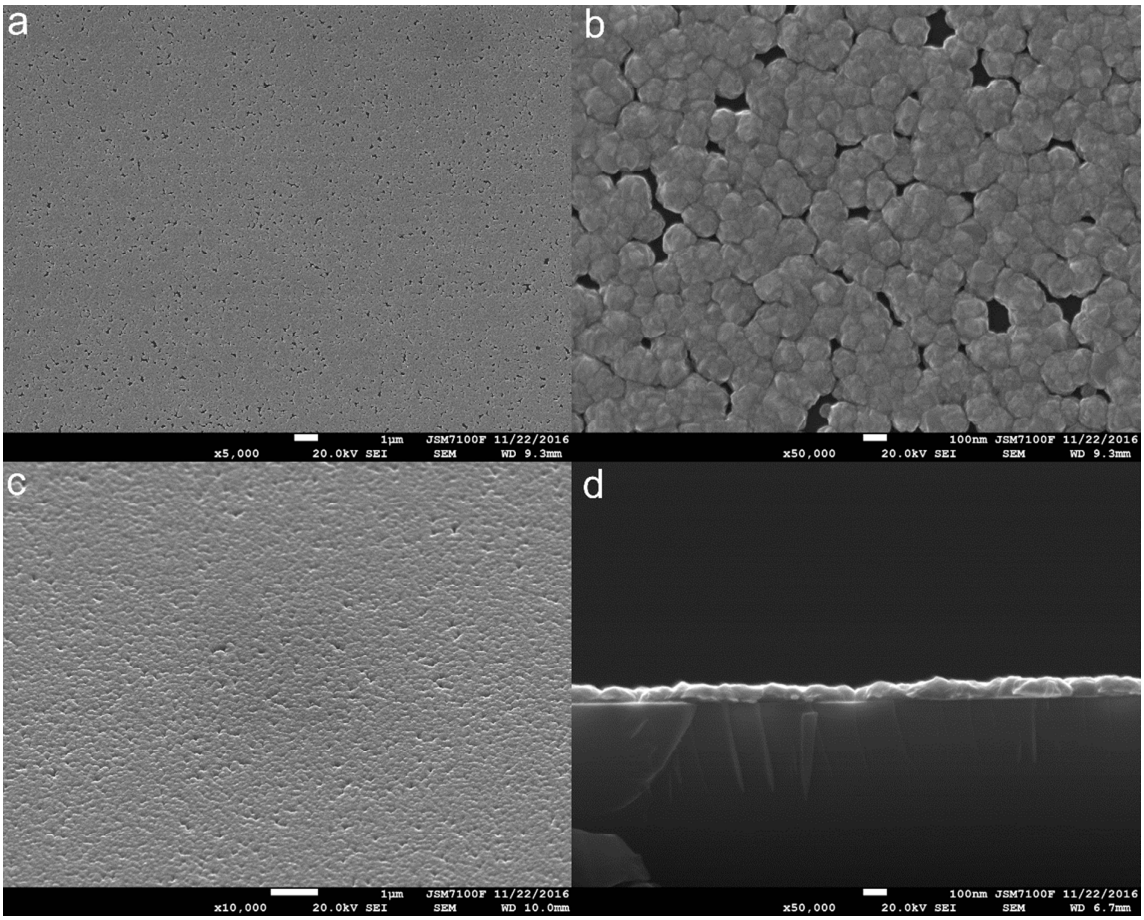

Figure S1. SEM pictures showing a *n*-Si surface that was coated with Ni by electrodeposition at -1.5 V vs SCE during 60 s (Q = -209 mC cm^{-2}). a,b) Top views. c) Tilted view (45 °). d) Cross-section.

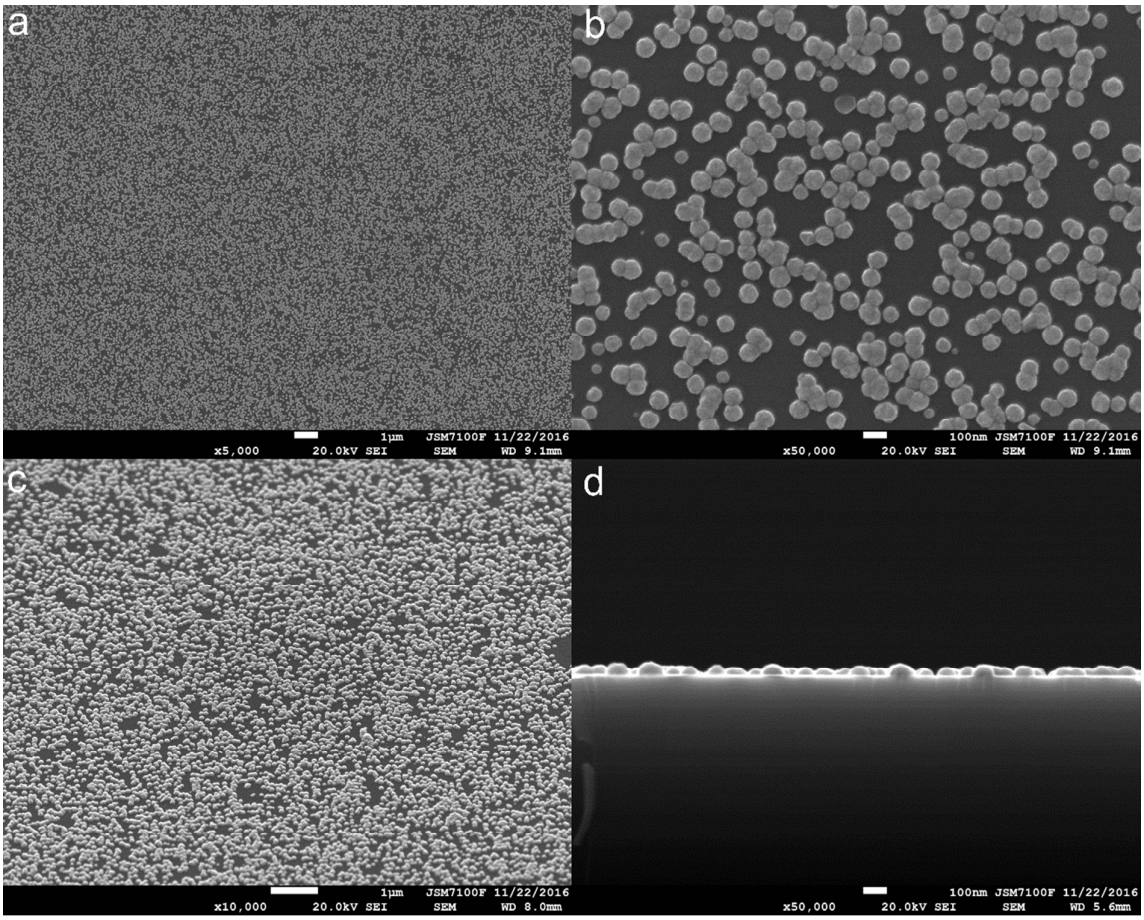

Figure S2. SEM pictures showing a *n*-Si surface that was coated with Ni by electrodeposition at -1.5 V vs SCE during 20 s (Q = -64 mC cm^{-2}). a,b) Top views. c) Tilted view (45 °). d) Cross-section.

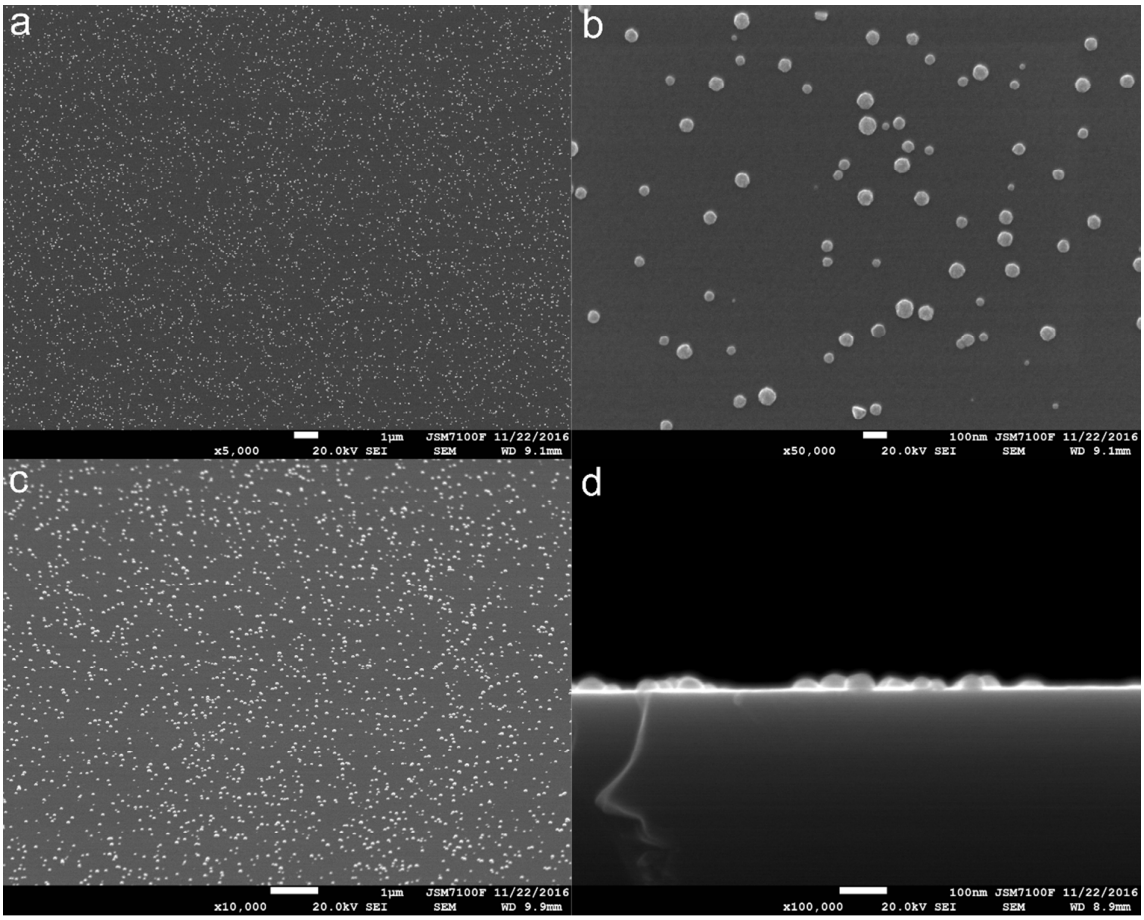

Figure S3. SEM pictures showing a *n*-Si surface that was coated with Ni by electrodeposition at -1.5 V vs SCE during 5 s (Q = -14 mC cm^{-2}). a,b) Top views. c) Tilted view (45 °). d) Cross-section.

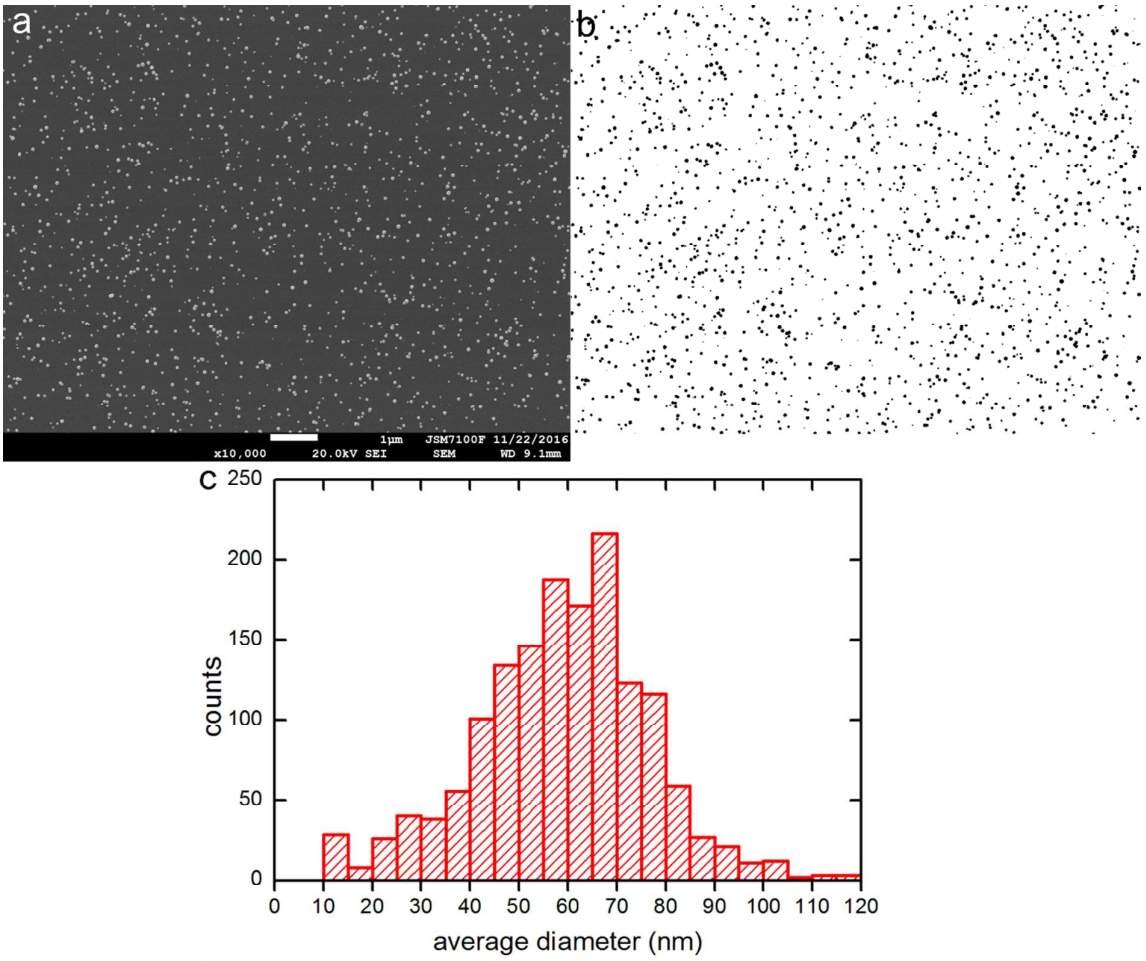

Figure S4. a) Original SEM picture of a *n*-Si surface that was coated with Ni by electrodeposition during 5 s and that was used to determine the size distribution. b) Corresponding binary picture used by the ImageJ freeware for particle analysis. c) Size distribution based on the analysis of Fig. S4b by ImageJ.

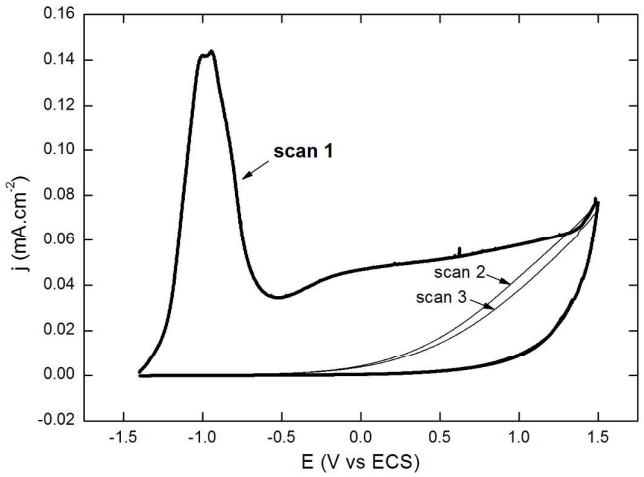

Figure S5. Cyclic voltammograms (three first scans) obtained for a HF-treated *n*-Si surface (non-metallized) under AM 1.5G illumination in 1 M NaOH. The scan rate is 20 mV s^{-1}.

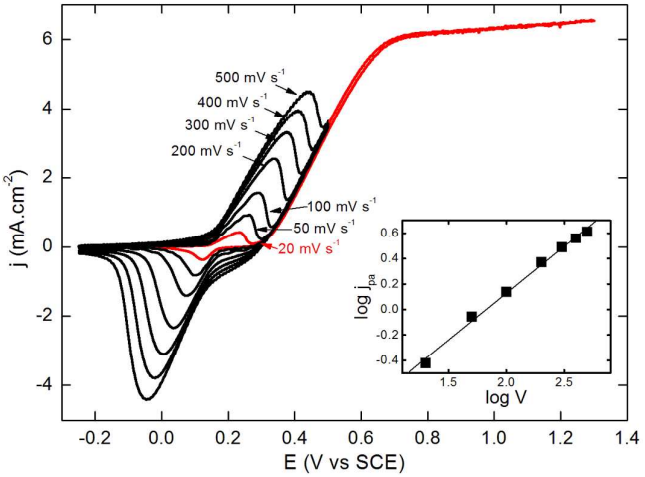

Figure S6. Cyclic voltammograms showing the influence of the scan rate on the Ni^{3+}/Ni^{2+} redox wave for a Ni-coated *n*-Si surface (consumed charge during electrodeposition: -277 mC cm^{-2}) under AM 1.5G illumination in 1 M NaOH. Inset: logarithmic plot of the current density of the anodic peak versus the scan rate. *The slope of 0.7 demonstrates that this redox process is behaving neither as purely diffusion-limited nor surface-confined. It would be rather consistent with a mixed control by both the oxidation of immobilized Ni^{2+} and the movement of protons through the material to the electrode-solution interface.*[7]

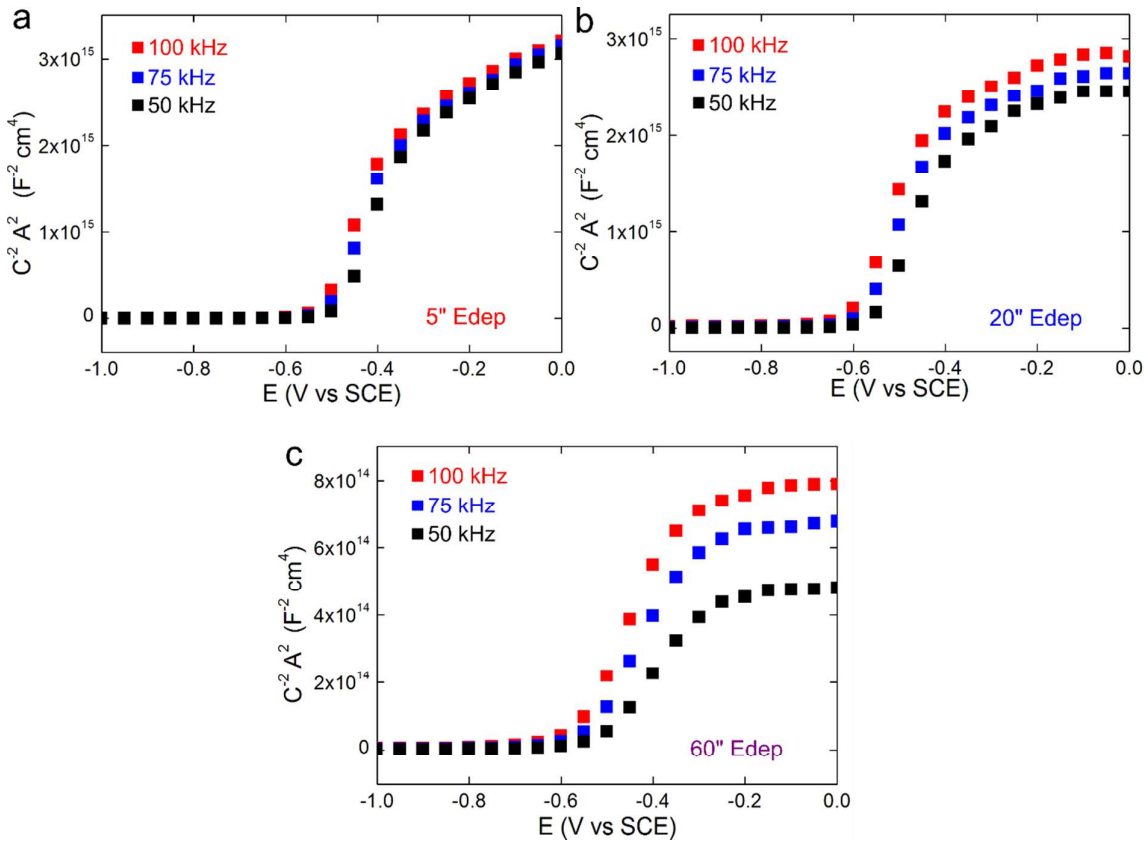

Figure S7. Mott-Schottky (MS) plots measured for Ni-coated *n*-Si for three electrodeposition times: a) 5 s, b) 20 s and c) 60 s. The measurements were performed in the dark in 1 M NaOH, sweeping the potential from positive to negative at 100 kHz (red squares), 75 kHz (blue squares) and 50 kHz (black squares).

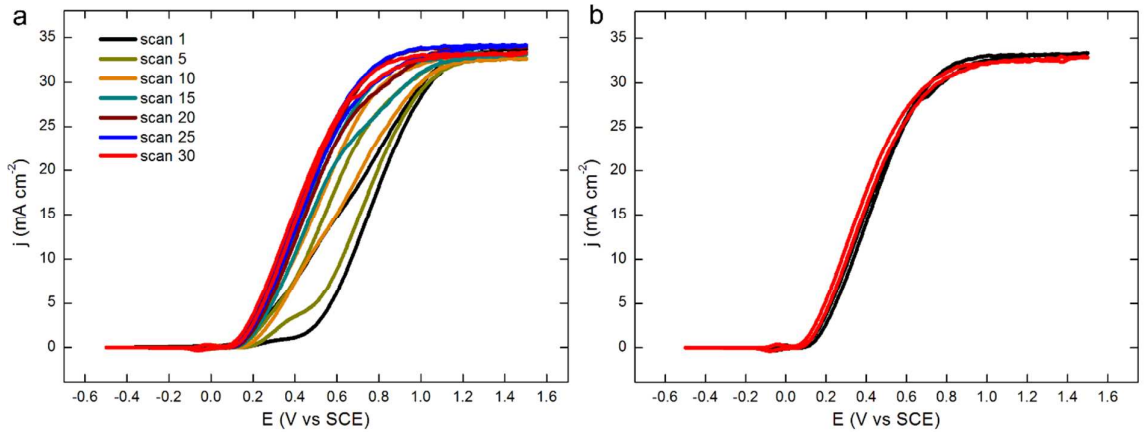

Figure S8. a) Consecutive cyclic voltammograms of a *n*-Si electrode coated with Ni by electrodeposition during 5 s. b) Cyclic voltammograms for the same electrode obtained before (black) and after (red) imposing +1 V vs SCE in 1 M NaOH under AM 1.5G illumination during 2 h. These CVs were recorded at 100 mV s^{-1} in 1 M NaOH under AM 1.5G illumination.

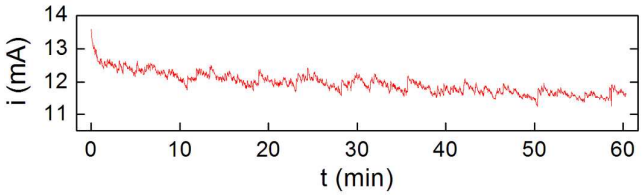

Figure S9. Chronoamperogram obtained during a preparative-scale electrolysis in the Hoffman cell, using a *n*-Si electrode coated with Ni by electrodeposition during 5 s (surface area = 0.38 cm^2), at +1 V vs SCE, in 1 M NaOH under AM 1.5G illumination.

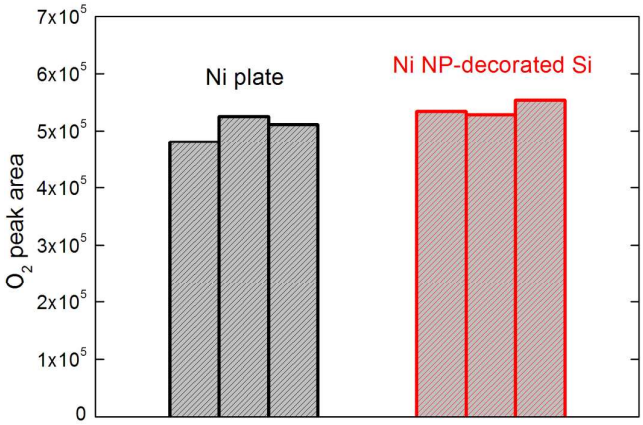

Figure S10. Graph showing the area values under the O_2 peak obtained by gas chromatography (injection volume of 50 µL) -*proportional to the amount of O_2 present in the headspace of the anolyte compartment*- after a preparative-scale electrolysis (consumed charge = +45 C) using a commercial Ni plate without illumination (black) and a *n*-Si electrode coated with Ni by electrodeposition during 5 s under AM 1.5G illumination (red). All these experiments were performed in the same electrochemical cell in 1 M NaOH (see the section "Preparative-scale electrolysis" for more details).

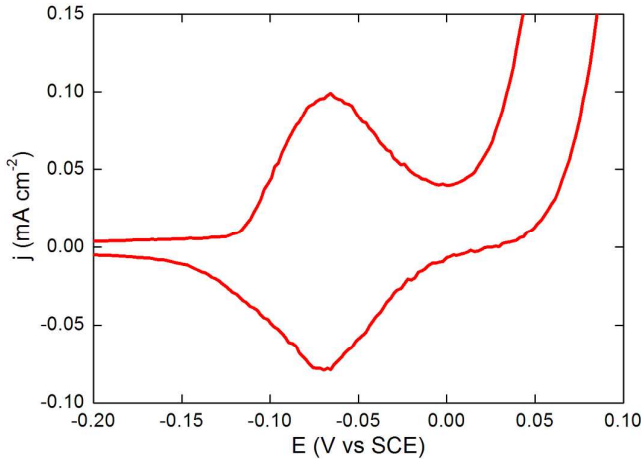

Figure S11. Detail of a cyclic voltammogram (showing the Ni^{3+}/Ni^{2+} redox wave) obtained for a *n*-Si electrode coated with Ni by electrodeposition during 5 s, under AM 1.5G illumination in 1 M NaOH at 20 mV s^{-1}.

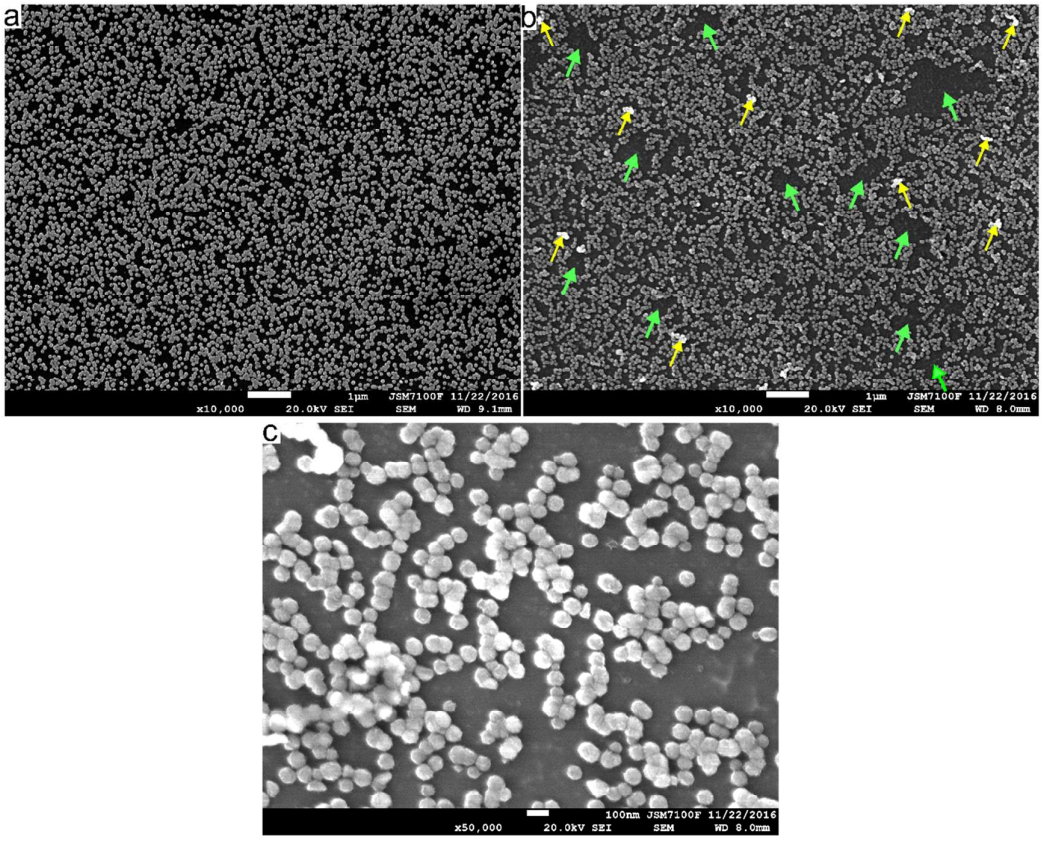

Figure S12. Top-view SEM picture showing the surface of a *n*-Si surface that was coated with Ni by electrodeposition at -1.5 V vs SCE during 20 s before (a) and after 25 h of preparative-scale electrolysis at +1 V vs SCE in 1 M NaOH under AM 1.5G illumination (b and c). Green arrows indicate areas were Ni NPs detached and yellow arrows indicate Ni NP clusters that have moved during the electrolysis.

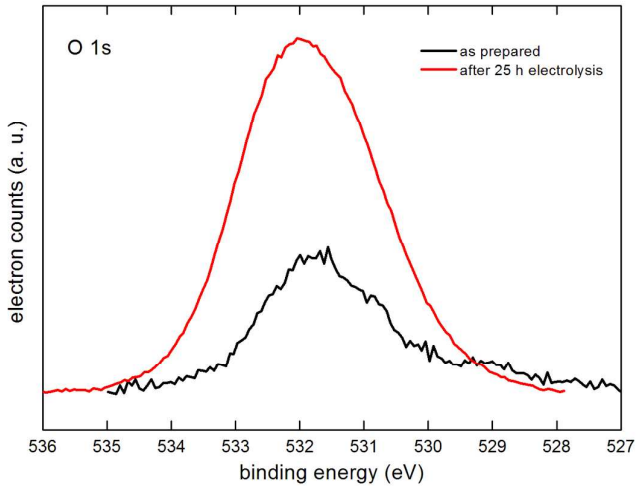

Figure S13. XPS spectra of the O 1s region for the *n*-Si surface coated with Ni by electrodeposition at -1.5 V vs SCE during 20 s (black line) and after ≈25 h of electrolysis (red line).

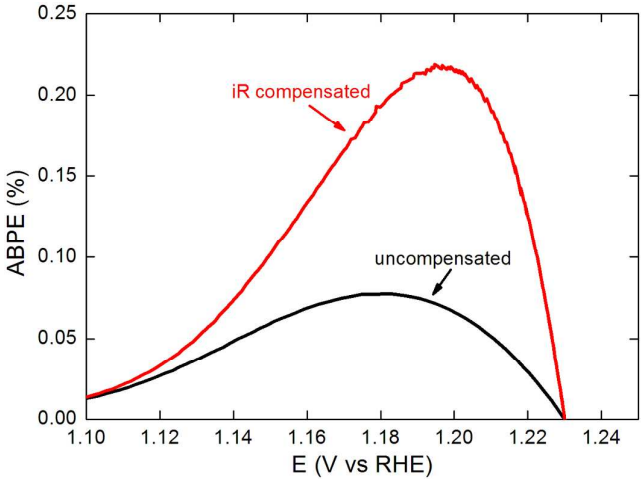

Figure S14. Curves showing the evolution of the applied bias photon-to-current efficiency (ABPE) as a function of the photoelectrode potential (*n*-Si coated with Ni by electrodeposition during 5 s) for the uncompensated *j*-*E* curve (black) and the ohmic drop-compensated *j*-*E* curve (red), (see Figure S16).

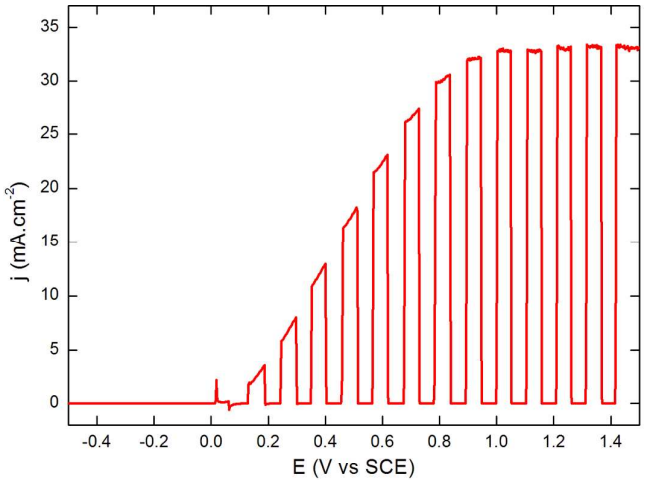

Figure S15. Linear sweep voltammogram (LSV) measured under chopped illumination (AM 1.5G) for *n*-Si coated with Ni for 5 s, recorded in 1 M NaOH at a sweep rate of 20 mV s^{-1}.

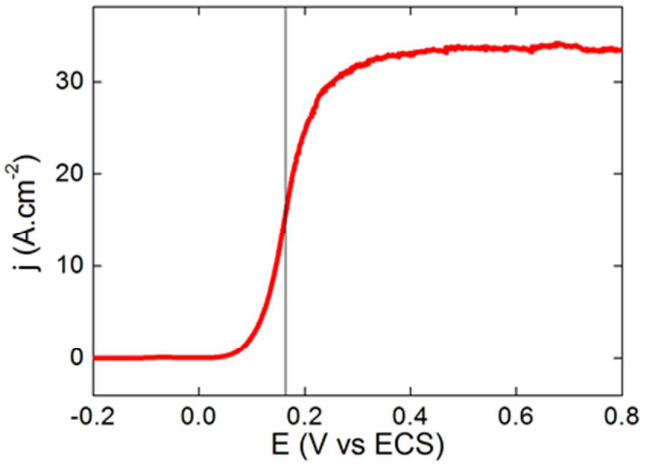

Figure S16. iR-compensated LSV for *n*-Si coated with Ni for 5 s, recorded in 1 M NaOH at a sweep rate of 20 mV s^{-1} under AM 1.5G illumination.

3. Supplementary tables

Table S1. Performances reported for OER using Si-based photoanodes coated with Ni-based materials and electrodeposited layers.

Ni-based coatings						
Substrate	**Coating Material** [a]	**Electrolyte**	**E_{onset} (V vs Ref)**	**j** [b] **(mA cm^{-2})**	**Stability time (h)**	**Reference**
n^+p-Si	sput. Ni	1 M KOH	0.25 (Hg/HgO)	≈ 43	3	Wang, J. Electroanal. Chem. 1987 [8]
n-Si	sol-gel NiOx	Buff. Na_2SO_4 (pH 7.25)	0.5 (Ag/AgCl)	6	0.5	Wang, Energy Environ. Sci. 2012 [9]
n-Si	e-beam evap. Ni	1 M KOH	1.07 (RHE)	10	12	Kenney, Science 2013 [6]
n-Si	e-beam evap. Ni	K-borate + Li borate	1.2 (RHE)	10	80	Kenney, Science 2013 [6]
textured *n*-Si	sput. $NiRuO_x$	buff. Na_2SO_4 (pH 7.25)	1 (RHE)	7	1.5	Wang, Nano Lett. 2013 [10]
np$^+$-Si	ALD TiO_2 / sput. Ni	1 M KOH	0.03 (SCE)	35	>100	Lewis, Science 2014 [11]
np$^+$-Si microwires	ALD TiO_2 / sput. $NiCrO_x$	1 M KOH	1.1 (RHE)	4.5	2200	Lewis, Energy Environ. Sci. 2014 [12]
HTJ-Si	sput. NiO_x	1 M KOH	0.9 (RHE)	34	200	Lewis, PNAS 2015 [13]
np$^+$-Si	sput. NiO_x	1 M KOH	0.9 (RHE)	34	1200	Lewis, J. Phys. Lett. 2015 [14]
np$^+$-Si	sput. $NiCo_2O_4$ / sput. NiFe	1 M KOH	1 (RHE)	31	72	Ager, J. Am. Chem. Soc. 2015 [15]
np$^+$-Si	sput. NiO_x / Edep. Fe	1 M KOH	1.05 (RHE)	15	300	Chorkendorff, J. Phys. Lett. 2016 [16]
n$^+$*pp*$^+$-Si	sput. $NiCoO_x$	1 M KOH	1.05 (RHE)	21	72	Chorkendorff, ChemElectroChem 2016 [17]
n-Si	ADL Al_2O_3 / e-beam evap. NiOx	1 M NaOH	1.3 (RHE)	9	20	Lee, Thin Solid Films 2016 [18]
n-Si	ALD TiOx / sput. ITO / Edep. NiOOH	1 M LiOH	0.9 (RHE)	15	< 2	Li, J. Am. Chem. Soc. 2016 [19]
Electrodeposited coatings						
Substrate	**Coating Material**	**Electrolyte**	**E onset (V vs Ref)**	**j** [b] **(mA cm^{-2})**	**Stability time (h)**	**Reference**
n-Si	Pt	0.2 M H_2SO_4	1.5 (NHE)	< 10	100	Bockris, Electrochimica Acta 1984 [20]
3jn-a-Si	Co-OEC	Borate buffer (pH 9.2)	-0.4 (RHE)	1.4	< 2	Nocera, Science 2014 [21]
n-Si	Co	1 M KOH	0.05 (Ag/AgCl)	35	≈2.5	Switzer, Nat. Mater. 2015 [22]
n-Si	Co	Borate buffer (pH 9)	0.5 (Ag/AgCl)	8	>125	Switzer, Nat. Mater. 2015 [22]
np$^+$*-Si*	Ni	1 M KOH	1 (RHE)	28	< 3	Shi, Adv. Energy Mater. 2016 [23]
np$^+$*-Si*	NiFe	1 M KOH	0.9 (RHE)	28	< 14	Shi, Adv. Energy Mater. 2016 [23]
np$^+$*-Si*	NiFe	Borate buffer (pH 9.5)	1 (RHE)	28	100	Shi, Adv. Energy Mater. 2016 [23]
n-Si	Ni	1 M NaOH	1.1 (RHE)	33	11.5	*This work*
n-Si	Ni	1 M NaOH	1.1 (RHE)	10	40.5	*This work*

[a] Sput.: sputtered, evap.: evaporated, ALD: atomic layer deposited, Edep.: electrodeposited. [b] Photocurrent density at the beginning of the stability test.

Table S2. Photoelectrochemical parameters for the Ni-coated Si photoanodes as a function of the doping type and the electrodeposition parameters.[a]

	electrodeposition parameters		E_{onset} [b]		η_{5mA}	j_{max}	photovoltage[c]	E_{fb}		stability[d]
	t (s)	Q (mC cm^{-2})	(V vs SCE)	(V vs RHE)	(V)	(mA cm^{-2})	(V)	(V vs SCE)	(V vs RHE)	(h)
p^{++}	5	-128	0.525	1.591	0.547	-	-	-	-	-
n	5	-14	0.050	1.116	0.034	33	0.513	-0.550	0.516	11.5
	20	-64	0.115	1.181	0.185	21	0.362	-0.605	0.461	25.0
	60	-209	0.280	1.346	0.452	10	0.095	-0.585	0.481	40.5

[a] t: electrodeposition time, Q: charge, E_{onset}: onset potential, η_{5mA}: overpotential required to obtain 5 mA cm^{-2}, j_{max}: light-limited photocatalytic current, E_{fb}: flat band potential. [b] Measured for j = 0.2 mA cm^{-2}. [c] Difference between η_{5mA} of the considered photoanode and Ni-coated p^{++} anode. [d] time when j reaches 0.7 j_{max}.

4. References

(1) Jia, Q.; Iwashina, K.; Kudo, A. *Proc. Natl. Acad. Sci.* **2012**, *109* (29), 11564.

(2) Loget, G.; Padilha, J. C.; Martini, E. A.; de Souza, M. O.; de Souza, R. F. *Int. J. Hydrog. Energy* **2009**, *34* (1), 84.

(3) McCrory, C. C. L.; Jung, S.; Ferrer, I. M.; Chatman, S. M.; Peters, J. C.; Jaramillo, T. F. *J. Am. Chem. Soc.* **2015**, *137* (13), 4347.

(4) Gonzalez-Elipe, A. R.; Munuera, G.; Espinos, J. P. *Surf. Interface Anal.* **1990**, *16* (1–12), 375.

(5) Trotochaud, L.; Ranney, J. K.; Williams, K. N.; Boettcher, S. W. *J. Am. Chem. Soc.* **2012**, *134* (41), 17253.

(6) Kenney, M. J.; Gong, M.; Li, Y.; Wu, J. Z.; Feng, J.; Lanza, M.; Dai, H. *Science* **2013**, *342* (6160), 836.

(7) Hall, D. S.; Bock, C.; MacDougall, B. R. *J. Electrochem. Soc.* **2013**, *160* (3), F235.

(8) Li, G.; Wang, S. *J. Electroanal. Chem. Interfacial Electrochem.* **1987**, *227* (1), 213.

(9) Sun, K.; Park, N.; Sun, Z.; Zhou, J.; Wang, J.; Pang, X.; Shen, S.; Noh, S. Y.; Jing, Y.; Jin, S.; Yu, P. K. L.; Wang, D. *Energy Environ. Sci.* **2012**, *5* (7), 7872.

(10) Sun, K.; Pang, X.; Shen, S.; Qian, X.; Cheung, J. S.; Wang, D. *Nano Lett.* **2013**, *13* (5), 2064.

(11) Hu, S.; Shaner, M. R.; Beardslee, J. A.; Lichterman, M.; Brunschwig, B. S.; Lewis, N. S. *Science* **2014**, *344* (6187), 1005 LP.

(12) Shaner, M. R.; Hu, S.; Sun, K.; Lewis, N. S. *Energy Environ. Sci.* **2015**, *8* (1), 203.

(13) Sun, K.; Saadi, F. H.; Lichterman, M. F.; Hale, W. G.; Wang, H.-P.; Zhou, X.; Plymale, N. T.; Omelchenko, S. T.; He, J.-H.; Papadantonakis, K. M.; Brunschwig, B. S.; Lewis, N. S. *Proc. Natl. Acad. Sci. USA* **2015**, *112* (12), 3612.

(14) Sun, K.; McDowell, M. T.; Nielander, A. C.; Hu, S.; Shaner, M. R.; Yang, F.; Brunschwig, B. S.; Lewis, N. S. *J. Phys. Chem. Lett.* **2015**, *6* (4), 592.

(15) Chen, L.; Yang, J.; Klaus, S.; Lee, L. J.; Woods-Robinson, R.; Ma, J.; Lum, Y.; Cooper, J. K.; Toma, F. M.; Wang, L.-W.; Sharp, I. D.; Bell, A. T.; Ager, J. W. *J. Am. Chem. Soc.* **2015**, *137* (30), 9595.

(16) Mei, B.; Permyakova, A. A.; Frydendal, R.; Bae, D.; Pedersen, T.; Malacrida, P.; Hansen, O.; Stephens, I. E. L.; Vesborg, P. C. K.; Seger, B.; Chorkendorff, I. *J. Phys. Chem. Lett.* **2014**, *5* (20), 3456.

(17) Bae, D.; Mei, B.; Frydendal, R.; Pedersen, T.; Seger, B.; Hansen, O.; Vesborg, P. C. K.; Chorkendorff, I. *ChemElectroChem* **2016**, *3* (10), 1546.

(18) Park, M.-J.; Jung, J.-Y.; Shin, S.-M.; Song, J.-W.; Nam, Y.-H.; Kim, D.-H.; Lee, J.-H. *Thin Solid Films* **2016**, *599*, 54.

(19) Yao, T.; Chen, R.; Li, J.; Han, J.; Qin, W.; Wang, H.; Shi, J.; Fan, F.; Li, C. *J. Am. Chem. Soc.* **2016**, *138* (41), 13664.

(20) Contractor, A. Q.; Bockris, J. O. *Electrochim. Acta* **1984**, *29* (10), 1427.

(21) Reece, S. Y.; Hamel, J. A.; Sung, K.; Jarvi, T. D.; Esswein, A. J.; Pijpers, J. J. H.; Nocera, D. G. *Science* **2011**, *334* (6056), 645 LP.

(22) Hill, J. C.; Landers, A. T.; Switzer, J. A. *Nat. Mater.* **2015**, *14* (11), 1150.

(23) Yu, X.; Yang, P.; Chen, S.; Zhang, M.; Shi, G. *Adv. Energy Mater.* **2016**, 1601805.